

Mathematical modeling of the solar sail spacecraft three-dimensional motion in heliocentric coordinate system

R.M. Khabibullin¹, O.L. Starinova¹

¹Samara National Research University, Moskovskoe Shosse 34A, Samara, Russia, 443086

Abstract. The paper outlines the mathematical motion model of the solar sail spacecraft. The work considers the mathematical three-dimensional motion model of the perfect-reflection solar sail and the operational orbit maintenance and correction algorithms in heliocentric coordinate system. On the basis of the formulated mathematical model the special software complex for interplanetary transfer simulation is developed. Especially, the mission of the transfer of the spacecraft from the Earth's orbit to the potentially hazardous asteroid is simulated. The obtained results during simulation demonstrate correctness and feasibility of the considered mathematical motion model.

Keywords: solar sail spacecraft, mathematical motion model, three-dimensional motion, heliocentric motion.

1. Introduction

Nowadays, there has been growing interest in missions to various planets of the Solar system. A promising way of cost reduction for such missions is the use of advanced physical principles of space travel such as movement by means of a solar sail. Solar sails are a form of spacecraft propulsion, which accelerate by means of pressure of stellar radiation on large ultra-thin mirrors. The possibility of saving a plenty of money has generated wide interest in the solar sailing technology. In recent years a considerable amount of work has been done in solar sailing. In the past five years great experience of the use of advanced physical principles of space travel such as movement by means of a solar sail has been obtained and described in [1]. The motion of a spacecraft on the Low Earth Orbit (LEO) is observed in [2]. Much less information is available about a flight of solar sail spacecraft to potentially hazardous asteroids. This paper considers a mathematical description of a research mission to near Earth asteroids. The aim of the present work is creation of a mathematical motion model of the solar sail spacecraft.

2. Mathematical motion model of the solar sail spacecraft

Solar sails are a form of spacecraft propulsion, which accelerate by means of pressure of stellar radiation on large ultra-thin mirrors. During interplanetary flight solar sail spacecraft moves under sunlight influence.

2.1. Mathematical motion model of the perfect-reflection solar sail

The two-dimensional motion model of the perfect-reflection solar sail is shown on Figure 1.

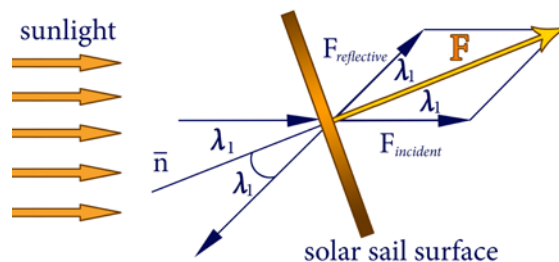


Figure 1. Solar sail spacecraft motion model.

Here $F_{incident}$ – propulsive power of incident photons, $F_{reflective}$ – propulsive power of incident photons, F – propulsive power of the solar pressure, \bar{n} – solar sail surface normal, λ_1 – control angle of solar sail spacecraft in the ecliptic. The control angle λ_2 appears in case of three-dimensional motion model of the perfect-reflection solar sail. The control angle λ_2 performs correction of a three-dimensional orbit elements such as inclination i and longitude of the ascending node Ω .

The three-dimensional motion equations in the heliocentric coordinate system is described by state variable vector

$$\bar{X} = (r, \phi, V_r, V_\phi, \Omega, i)^T, \tag{1}$$

or by the system of differential equations [4]

$$\begin{cases} \dot{r} = V_r \\ \dot{\phi} = \frac{V_\phi}{r} - \frac{a_0 \cdot \sin(\lambda_2)}{V_\phi \cdot \tan(\Omega)} \\ \dot{V}_r = \frac{V_\phi^2}{r} - \frac{1}{r^2} + a_0 \cdot \cos(\lambda_1) \cdot \cos(\lambda_2) \\ \dot{V}_\phi = -\frac{V_r \cdot V_\phi}{r} + a_0 \cdot \sin(\lambda_1) \cdot \cos(\lambda_2) \\ \dot{\Omega} = \frac{a_0 \cdot \sin(\phi) \cdot \sin(\lambda_2)}{\sin(i) \cdot V_\phi} \\ \dot{i} = \frac{a_0 \cdot \cos(\phi) \cdot \sin(\lambda_2)}{V_\phi} \end{cases} \tag{2}$$

where r is distance of spacecraft and Sun centers of mass, ϕ is argument of latitude, V_r is radial velocity of a spacecraft, V_ϕ is transversal velocity of a spacecraft, Ω is longitude of the ascending node, i is inclination of orbit, a_0 is complex acceleration, λ_1 is control angle of solar sail spacecraft in the ecliptic plane (angle between solar sail surface normal and radius vector), λ_2 is control angle performs maintenance and correction of inclination i and longitude of ascending node Ω (angle between solar sail surface normal and radius vector).

The complex acceleration is determined as:

$$a_0 = \frac{F}{m} = \frac{2 \cdot S_r \cdot S \cdot \cos(\lambda_1) \cdot \cos(\lambda_2)}{c \cdot m}, \tag{3}$$

where F is propulsive power of the solar pressure, m is mass of a spacecraft, S_r is energy of solar electromagnetic wave which strike upon surface unit, S is current sail spread, c is velocity of light.

The propulsive power of the solar pressure is determined as:

$$F = F_{incident} + F_{reflective} = \frac{S_r}{c} \cdot S(\lambda_1) \cdot \cos(\lambda_1) + \varepsilon \cdot \frac{S_r}{c} \cdot S(\lambda_1) \cdot \cos(\lambda_1), \tag{4}$$

where

$$S(\lambda_1) = S \cdot \cos(\lambda_1) \tag{5}$$

2.2. Operational orbit maintenance and correction algorithms

The orbital elements of a three-dimensional motion are shown on Fig. 4. Here i is inclination, r is distance of spacecraft and Sun centres of mass, ϑ is true anomaly, ω is perihelion argument, Ω is longitude of the ascending node, u is argument of latitude.

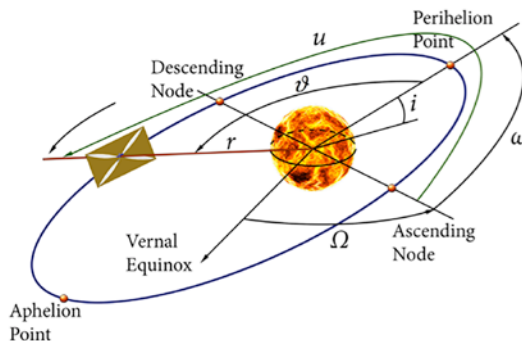


Figure 2. Orbital elements of a three-dimensional motion.

The algorithms of the operational orbit maintenance and correction are designed to control of a solar sail spacecraft on an operational orbit. The algorithms are based on the law of the Keplerian element changes. In [3] the law of the Keplerian element changes is following:

$$\frac{dK}{dt} = f_1(\vartheta) \cdot \cos^3(\lambda_1) + f_2(\vartheta) \cdot \cos^2(\lambda_1) \cdot \sin(\lambda_1) \tag{6}$$

The equation of motion (6) allows us to estimate locally optimal control laws for a solar sail spacecraft. The locally optimal control laws provide maintenance and correction of the orbital elements.

According to Figure 2 and (6) the locally optimal control law components f_1 and f_2 of the equation of motion were found. Table 1 shows the components of orbit parameter increment. The components of orbit parameter decrement and components of orbit parameter maintenance are demonstrated in table 2 and table 3 respectively.

Table 1. Locally optimal control law components of orbit parameter increment.

№	Name	Components f_1 and f_2	
1	parameter increment, p	0	$\frac{1}{1 + e \cdot \cos(\vartheta)}$
2	semi-major axis increment, a	$e \cdot \cos(\vartheta)$	$-1 + e \cdot \cos(\vartheta)$
3	eccentricity increment, e	$\sin(\vartheta)$	$\frac{e \cdot \cos^2(\vartheta) + 2 \cdot \cos(\vartheta) + e}{1 + e \cdot \cos(\vartheta)}$
4	perihelion radius increment, r_π	$-\sin(\vartheta)$	$-\frac{2 \cdot (1 - \cos(\vartheta)) + e \cdot \sin^2(\vartheta)}{1 + e \cdot \cos(\vartheta)}$
5	aphelion radius increment, r_α	$\sin(\vartheta)$	$\frac{2 \cdot (1 + \cos(\vartheta)) - e \cdot \sin^2(\vartheta)}{1 + e \cdot \cos(\vartheta)}$
6	perihelion argument increment, ω	$-\cos(\vartheta)$	$-\frac{\sin(\vartheta) \cdot (2 + e \cdot \cos(\vartheta))}{1 + e \cdot \cos(\vartheta)}$
7	inclination increment, i	$\frac{\sin(u)}{\sin(i)} > 0,$	$\sin(2\lambda_2) = 1$
8	longitude of the ascending node increment, Ω	$\cos(u) > 0,$	$\sin(2\lambda_2) = 1$

Table 2. Locally optimal control law components of orbit parameter decrement.

№	Name	Components f_1 and f_2	
1	parameter decrement, p	0	$\frac{1}{1 + e \cdot \cos(\mathcal{G})}$
2	semi-major axis decrement, a	$e \cdot \cos(\mathcal{G})$	$1 + e \cdot \cos(\mathcal{G})$
3	eccentricity decrement, e	$\sin(\mathcal{G})$	$\frac{e \cdot \cos^2(\mathcal{G}) + 2 \cdot \cos(\mathcal{G}) + e}{1 + e \cdot \cos(\mathcal{G})}$
4	perihelion radius decrement, r_π	$-\sin(\mathcal{G})$	$\frac{2 \cdot (1 - \cos(\mathcal{G})) + e \cdot \sin^2(\mathcal{G})}{1 + e \cdot \cos(\mathcal{G})}$
5	aphelion radius decrement, r_α	$\sin(\mathcal{G})$	$-\frac{2 \cdot (1 + \cos(\mathcal{G})) - e \cdot \sin^2(\mathcal{G})}{1 + e \cdot \cos(\mathcal{G})}$
6	perihelion argument decrement, ω	$-\cos(\mathcal{G})$	$-\frac{\sin(\mathcal{G})(2 + e \cdot \cos(\mathcal{G}))}{1 + e \cdot \cos(\mathcal{G})}$
7	inclination decrement, i	$\frac{\sin(u)}{\sin(i)} < 0,$	$\sin(2\lambda_2) = -1$
8	longitude of the ascending node decrement, Ω	$\cos(u) < 0,$	$\sin(2\lambda_2) = -1$

Table 3. Locally optimal control law components of orbit parameter maintenance.

№	Name	Components f_1 and f_2	
1	parameter maintenance, p	$\frac{1}{1 + e \cdot \cos(\mathcal{G})}$	0
2	semi-major axis maintenance, a	$1 + e \cdot \cos(\mathcal{G})$	$e \cdot \cos(\mathcal{G})$
3	eccentricity maintenance, e	$\frac{e \cdot \cos^2(\mathcal{G}) + 2 \cdot \cos(\mathcal{G}) + e}{1 + e \cdot \cos(\mathcal{G})}$	$\sin(\mathcal{G})$
4	perihelion radius maintenance, r_π	$\frac{2 \cdot (1 - \cos(\mathcal{G})) + e \cdot \sin^2(\mathcal{G})}{1 + e \cdot \cos(\mathcal{G})}$	$-\sin(\mathcal{G})$
5	aphelion radius maintenance, r_α	$\frac{2 \cdot (1 + \cos(\mathcal{G})) - e \cdot \sin^2(\mathcal{G})}{1 + e \cdot \cos(\mathcal{G})}$	$\sin(\mathcal{G})$
6	perihelion argument maintenance, ω	$\frac{\sin(\mathcal{G}) \cdot (2 + e \cdot \cos(\mathcal{G}))}{1 + e \cdot \cos(\mathcal{G})}$	$-\cos(\mathcal{G})$
7	inclination maintenance, i	$\lambda_2 = 0$	
8	longitude of the ascending node maintenance, Ω	$\lambda_2 = 0$	

3. Simulation findings

On the basis of the formulated mathematical model the special software for interplanetary transfer simulation is developed. The paper describes findings of the solar sail spacecraft motion simulation to demonstrate efficiency of the algorithms of the operational orbit maintenance and correction. In this part of paper the flight to the potentially hazardous asteroid 433 Eros from Earth orbit is considered.

The solar sail spacecraft starts from the Earth’s orbit. The suppositions, which are used during simulation session, include following points:

- Earth escape is executed by means of booster;
- initial orbit state variables of spacecraft align with Earth state variables on the date of start;
- control angle λ_1 is constant;
- the aim of the simulated mission is ascent to the asteroid orbit.

The findings of the simulation demonstrate that solar sail spacecraft is capable to ascent to 433 Eros orbit during 2291 days.

4. Conclusion

The main purpose of this paper has been to investigate an advanced physical principle of space travel such as solar sailing. Our mathematical motion model and findings demonstrate a capability of the use of a solar sail for ascent to the orbit of the asteroid 433 Eros. The results of flight simulation indicate that the algorithms of the operational orbit maintenance and correction can help solar sail spacecraft be transferred to a potentially hazardous asteroid orbit.

5. References

- [1] Gorbunova I.V. Control of the spacecraft with a solar sail, performing an interplanetary flight / I.V. Gorbunova, O.L. Starinova // 7th International Conference on Recent Advances in Space Technologies, IEEE Conference publications. – 2015. – P.111-115.
- [2] Ishkov, S.A. Optimization and modeling of movement with the solar sail / S.A. Ishkov, O.L. Starinova // Izvestiya of Samara Scientific Center Russian Academy of Sciences. – 2005. – Vol. 7(13). – P. 99-106.
- [3] Starinova, O. Analytical control laws of the heliocentric motion of the solar sail spacecraft / O. Starinova, I. Gorbunova // 10th International Conference on Mathematical Problems in Engineering, AIP Conference Proceedings. – 2014. – Vol. 1637. – P. 358-367.